



The mirror symmetric centroid difference method for picosecond lifetime measurements via γ – γ coincidences using very fast LaBr₃(Ce) scintillator detectors

J.-M. Régis*, G. Pascovici, J. Jolie, M. Rudigier

Institut für Kernphysik, Universität zu Köln, Zùlpicher Str. 77, 50937 Köln, Germany

ARTICLE INFO

Article history:

Received 24 March 2010

Received in revised form

29 June 2010

Accepted 16 July 2010

Available online 23 July 2010

Keywords:

Fast timing

Lifetime measurements

LaBr₃(Ce) scintillator

Centroid shift method

MSCD method

ABSTRACT

The ultra-fast timing technique was introduced in the 1980s and is capable of measuring picosecond lifetimes of nuclear excited states with about 3 ps accuracy. Very fast scintillator detectors are connected to an electronic timing circuit and detector vs. detector time spectra are analyzed by means of the centroid shift method. The very good 3% energy resolution of the nowadays available LaBr₃(Ce) scintillator detectors for γ -rays has made possible an extension of the well-established fast timing technique. The energy dependent fast timing characteristics or the prompt curve, respectively, of the LaBr₃(Ce) scintillator detector has been measured using a standard ¹⁵²Eu γ -ray source. For any energy combination in the range of 200 keV < E _{γ} < 1500 keV, the γ - γ fast timing characteristics is calibrated as a function of energy with an accuracy of 2–4 ps. An extension of the centroid shift method providing very attractive features for picosecond lifetime measurements is presented. The mirror symmetric centroid difference method takes advantage of the symmetry obtained when performing γ - γ lifetime measurements using a pair of almost identical very fast scintillator detectors. In particular cases, the use of the mirror symmetric centroid difference method also allows the direct determination of picosecond lifetimes, hence without the need of calibrating the prompt curve.

© 2010 Elsevier B.V. All rights reserved.

1. Introduction

The determination of lifetimes of nuclear excited states is very important for the test of theoretical models describing nuclear structure. Nuclear excited state lifetimes in the range of a few femtoseconds to microseconds and more are intensively studied, but most of the lifetimes found are in the picosecond region. Fundamental works in the nowadays widely applied ultra-fast timing technique were carried out by Mach et al. [1,2] and Moszyński et al. [3,4]. The technique relies on β - γ coincidences using very fast organic and heavy inorganic scintillator detectors to access lifetimes of nuclear excited states in the few picosecond region. The challenge is to calibrate the energy dependent centroid position of prompt events yielding the prompt response function (PRF) describing the setup timing characteristics, also known as the “prompt curve”, which is needed for lifetime determination by means of the centroid shift method.

The ultra-fast timing technique applied on only γ - γ -coincidences is very interesting for in-beam experiments. Three dimensional energy–energy–time matrices can be built to

perform the well-known generalized centroid shift method [5,6]. The here presented Mirror Symmetric Centroid Difference (MSCD) method is similar to this method, but uses both energy axes to obtain a combination of two time distributions, whose centroid difference has a very attractive mirror symmetry.

Recently, a new generation of heavily doped inorganic scintillators has been developed. For the LaBr₃(Ce) scintillators, an increase in Cerium doping is equivalent to an increase in energy and time resolution [7]. The timing property is almost equivalent to very fast plastic scintillators, while the energy resolution of 3% [4] improves remarkably the peak to background ratio. This enables the introduction of a new picosecond γ - γ timing technique.

2. Fast timing considerations

For the purpose of investigating the overall timing properties of a standard fast timing setup (Fig. 1), we investigated the intrinsic timing characteristics of each individual timing branch. The scintillator detector assembly consists of a cylindrically shaped \varnothing 1.5 in. \times 1.5 in. LaBr₃(Ce) scintillator in conjunction with the XP20D0 photomultiplier (PM). Compared with previously used XP2020 PM, the PM anode timing of the

* Corresponding author. Tel.: +49 221 4703622; fax: +49 221 4705168.
E-mail address: regis@ikp.uni-koeln.de (J.-M. Régis).

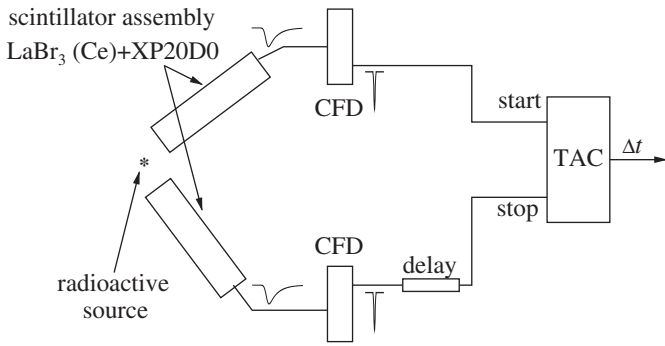


Fig. 1. Schematic draw of the γ - γ fast timing setup used in this work.

XP20D0 is improved by factor of 1.2, due to the application of a screening grid at the anode and the reduced number of dynodes [4]. The two scintillator and PM assemblies were adjusted to deliver almost identical transfer functions, i.e. same amplitude vs. energy characteristics. As shown in Fig. 1, the PM anode signal from the scintillator assembly was directly connected to the input of a Constant Fraction Discriminator (CFD, model Ortec 584). The proper adjustments of the CFD is a major issue, while the main property of the CFD is to minimize the timing walk variation on the amplitude of the input signal. The Time to Amplitude Converter (TAC) output amplitude is proportional to the time difference between the two fast CFD timing signals coupled directly at the start and delayed at the stop inputs. The TAC output amplitude spectrum linearity and TAC time resolution were investigated by the use of Ortec 462 high precision time calibrator. The TAC time distribution is a symmetric Gaussian distribution with FWHM of 12 ps. To guarantee wide TAC linearity for both timing branches, the delay of the stop branch was chosen such that the TAC time distribution was placed in the middle of the TAC range. All passive electronic components including coaxial cables have been tested carefully to avoid possible systematic uncertainties.

A slow energy coincidence circuit completed the setup to record triple events ($E_1, E_2, \Delta t_{12}$) within a coincidence window of about 100 ns. For this work, the events were stored in 1 h runs in order to investigate for shifts in energy and in time. A count rate dependent energy shift with magnitude of the order of $\leq 1\%/h$ was observed. Taking these energy shifts into account, the energy gated time spectra are stable in time. However, in some cases, a time shift as a result of thermal fluctuations in electronics could also be observed. After more than 30 h of measurement, this energy independent time shift can be slightly larger than 10 ps.

2.1. Time resolution of the fast timing setup

The time resolution of the whole fast timing setup is mainly caused by the structure of the scintillator detector rise time, which can be divided in two parts. Firstly, the contribution due to the nature of the scintillator and secondly, the timing performance of the PM. An important factor is the lifetime of the excited states in the crystal which decay by the emission of scintillation light. Very fast scintillators have decay times in the few nanosecond region. The crystal size can be important, because of the interaction point vs. scintillation light collection time dependency of 33 ps/cm [1,3]. A high scintillation light output is desirable for good PM timing performance, which depends on several parameters, as the number of photo electrons released at the photo cathode, their time spread to the first dynode and the spread in the electron multiplier gain [4]. For different crystal types, the nowadays available multi-stage PMs differ only slightly

in rise times and are superior to typical scintillator decay times [4,8]. Due to total detector assembly rise time, the time resolution of the $\varnothing 1$ in. \times 1 in. cylindrical $\text{LaBr}_3(\text{Ce})$ scintillator in conjunction with the XP20D0 PM is slightly larger than 200 ps [4] (FWHM for 511 keV annihilation lines in ^{22}Na). The CFD also contributes to the time resolution of the setup. This is due to its time walk and time jitter, which can become important for low energies corresponding to $E_\gamma < 300$ keV.

The intrinsic time resolution of the setup can be measured using prompt decays. For fast timing setups, a prompt decay is associated with lifetimes $\tau < 1$ ps. The obtained prompt response function (PRF) is a Gaussian distribution and its FWHM includes all timing uncertainties obtained from the scintillator and PM physics, electronics and setup geometry.

In the ideal case of no feeding and no background contributions, time distributions of directly measurable lifetimes show a typical asymmetric shape of a convolution of the energy dependent PRF $P(t)$ with an exponential decay:

$$D(t) = n\lambda \int_{-\infty}^t P(x)e^{-\lambda(t-x)} dx, \quad \lambda = 1/\tau \quad (1)$$

where n is the normalization factor. Time distributions of lifetimes which are longer than the FWHM of the energy corresponding PRF have a pronounced slope and the lifetime τ can be determined directly using the slope or the deconvolution method according to Eq. (1) [1,9,10].

Often, the setup time resolution is expressed by the FWHM of the PRF, which is energy dependent. Using the deconvolution method, the time resolution is rather given by the smallest slope that can be deconvoluted. For γ - γ setups with detectors at equal distances to the γ -ray source, the time resolution can be expressed by $\sigma_\tau = \ln(2) \cdot \text{FWHM}$ [1].

2.2. The centroid shift method

The centroid shift method is used for determination of lifetimes which are smaller than the setup time resolution. The centroid, i.e. the first moment of a delayed time distribution $D(t)$ is defined as

$$C(D) = \langle t \rangle = \frac{\int tD(t) dt}{\int D(t) dt} \quad (2)$$

with $D(t)$ of Eq. (1). The statistical error is given by the variance of $D(t)$

$$dC = \sqrt{\text{var}[D(t)]} = \sqrt{\langle t^2 \rangle - \langle t \rangle^2}. \quad (3)$$

Assuming the ideal case of no feeding and no background contributions, it follows per definition that the lifetime τ is directly given by the difference of the centroids of the delayed time distribution and the prompt time distribution corresponding to the energy gates of the delayed one:

$$\tau = C(D) - C(P). \quad (4)$$

The knowledge of the setup timing characteristics, i.e. the energy dependent PRF centroid $C(P)$, is crucial for centroid shift analysis and its accuracy gives the limit of the fast timing technique.

2.3. The prompt curve determination

The uncertainty in determining the ultra-fast PRF centroid is a question of statistics and can be better than 1 ps. The main problem, however, is that the PRF centroid is energy dependent and has to be interpolated for the energy of interest [1]. In principle, the walk-energy dependence of the detector signal is inherently compensated by the CFD method itself, but the fast

timing signal delivered at the CFD output still has an amount of time walk, which is amplitude dependent.

The CFD principle is to shape the input signal to generate a bipolar signal, its zero-crossing is used as a trigger to produce the fast CFD output timing signal [11]. By proper selection of the CFD shaping delay time t_d , the walk due to rise time and amplitude variations of the input signals can be minimized. In principle, the best timing with very fast scintillator detectors is obtained for the so-called true-constant-fraction (TCF) condition $t_d > t_r(1-f)$ [11], where t_r is the detector signal rise time and f is the attenuation factor ($f=0.2$ for the Ortec 584), that defines the triggering fraction. In this work, we present the results obtained using the amplitude-and-rise-time-compensation timing mode (ARC) with the condition $t_d < t_r(1-f)$. In any case, the experimentally obtained walk has to be determined in the off-line analysis in order to deduce the lifetime from the experimental data according to Eq. (4).

In the off-line analysis, one has to struggle with prompt and/or delayed coincidence contributions from the background which contaminate the time distribution of interest. The background contributions result in a shift of the total time distribution compared to the net time distribution. This shift can be derived using the Compton correction procedure described in Refs. [1–3]. The non-linear energy dependent PRF centroid which defines the prompt curve (often called “the walk characteristics”) is then interpolated using measurements of several prompt time distributions at different energies covering a wide dynamic range.

3. The timing characteristics of the LaBr₃(Ce) scintillator detector

To measure the prompt curve of the LaBr₃(Ce) scintillator detector in a γ - γ fast timing experiment, a walk free reference timing signal from the experimental system is needed. This is achieved by gating one γ -ray detector constantly on a directly populating or depopulating transition of interest. The other detector selects coincident prompt transitions of different energies to measure its prompt curve. In the off-line analysis, this work has to be made for every single γ -ray detector in order to gain in statistics when performing γ - γ lifetime experiments using arrays of detectors.

The setup for our experiment consisted of two LaBr₃(Ce) scintillator detectors placed at equal distances (3 cm) from a γ -ray source and with an angle of 120 degrees in between them. The standard ^{152}Eu γ -ray source produces many coincident transitions connecting a lot of states with precisely known picosecond lifetimes which is ideal to measure the prompt curve according to Eq. (4).

As a good example, we consider the 344 keV state in ^{152}Gd (a portion of the level scheme is shown in Fig. 2). As seven γ -ray transitions are in coincidence with the 344 keV decay transition, the reference energy gate of 344 keV is used to provide the walk free reference timing signal of the setup, in this case delivered by the stop detector. Fig. 3 shows the coincidence spectrum of ^{152}Gd obtained by gating on the 344 keV decay transition. Due to the very good energy resolution of the LaBr₃(Ce) scintillator detectors, the transitions are well separated.

The time spectra of the 344 keV decay transition presented in Fig. 4 were obtained without subtracting background contributions of any kind. A very small asymmetry on the stop side (on the right) of the time distributions is observed which is due to the lifetime of the 2_1^+ state in ^{152}Gd . The asymmetry is too small for being used to determine the lifetime directly, according to Eq. (1). The energy dependent time resolution is given by the FWHM of the time spectra. Note the energy dependent time

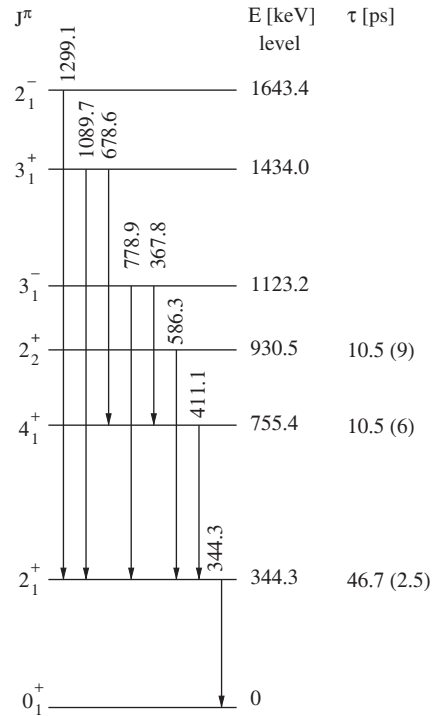


Fig. 2. Partial level scheme of ^{152}Gd obtained after β^+ decay of the standard ^{152}Eu γ -ray source. J^π , E_γ , E_{level} and τ from Ref. [12].

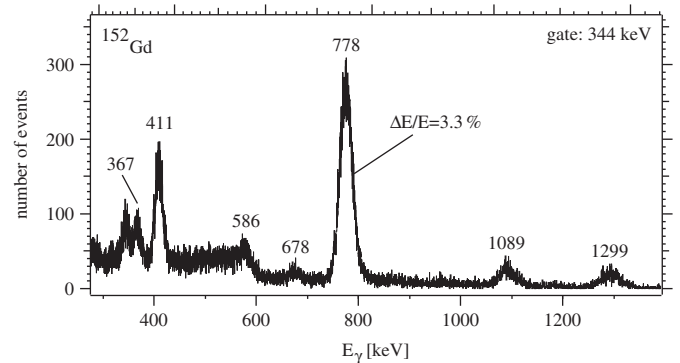


Fig. 3. Coincidence γ -ray spectrum of the LaBr₃(Ce) scintillator detector obtained by gating on the 344 keV transition of ^{152}Gd .

distribution centroids which were determined with a statistical accuracy of only 2–7 ps. The 344 keV gated centroids of coincident transitions were plotted against the γ -ray energy to obtain the centroid curve, i.e. the 344 keV gated prompt curve shifted by the lifetime τ , as presented in Fig. 5. The centroids at 367 and 678 keV were corrected for the lifetime of the intermediate 4_1^+ state in ^{152}Gd . The variation of the centroids with energy is very smooth and could be described as a function of energy. The centroids were fitted using the calibration function:

$$C(E_\gamma) = \frac{a}{E_\gamma + b} + c \quad (5)$$

with a , b and c being free fit parameters with resulting values of

$$a = -(182.6 \pm 15.3) \times 10^3 \text{ keV chn} \quad (8.4\%)$$

$$b = (577 \pm 51) \text{ keV} \quad (8.8\%)$$

$$c = (4927 \pm 6) \text{ chn} \quad (0.2\%).$$

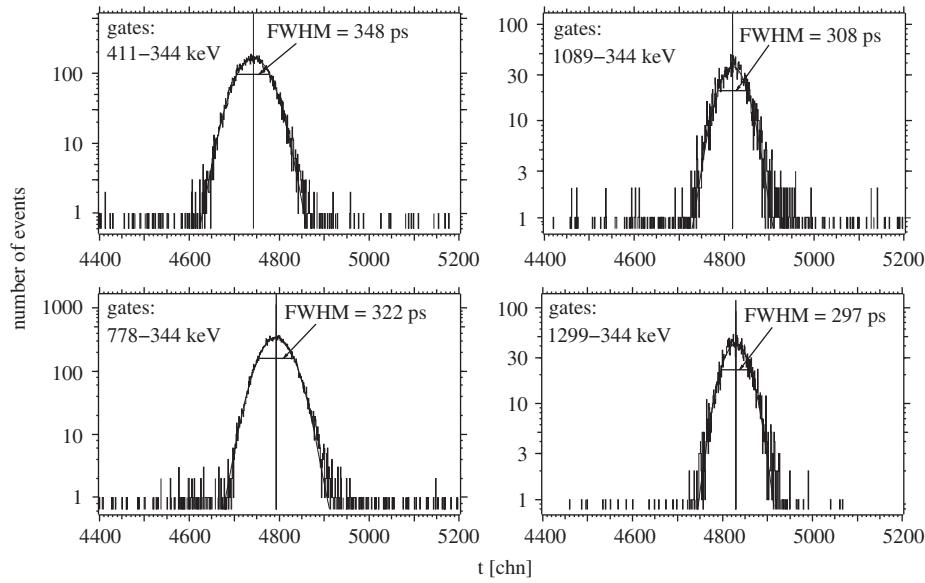


Fig. 4. $\text{LaBr}_3(\text{Ce})$ γ – γ time distributions of the 2_1^+ state in ^{152}Gd obtained by gating the decaying 344 keV transition (on the delayed detector giving the stop signal for the TAC) and direct feeders of different energies (see also Fig. 3). The spectrum calibration is 4.25 ps/chn. Centroid positions are illustrated by a vertical line.

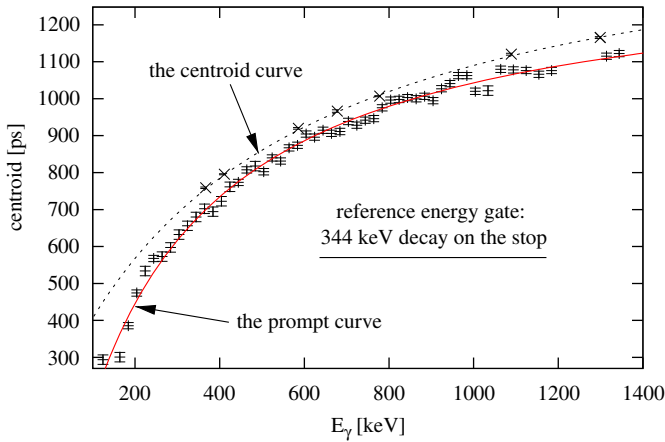


Fig. 5. Centroids of the 344 keV decay transition in ^{152}Gd (gated on the stop detector) in dependence on gated γ –ray energy. The dashed curve was obtained by a fit of the data points using Eq. (5) and represents the 344 keV gated centroid curve. The approximated prompt curve was obtained using the Compton continuum of the prompt ^{60}Co source by gating the stop detector at 344 keV and varying the Compton gates on the start detector.

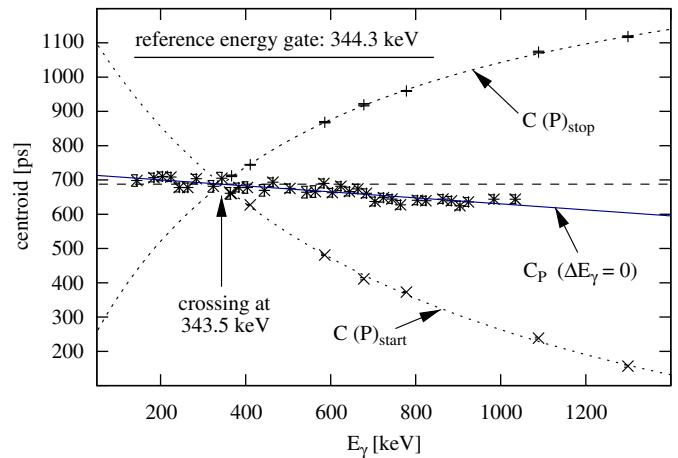


Fig. 6. The 344 keV gated prompt curves (the dashed curves) of the two timing branches obtained by fitting the lifetime corrected full energy centroids using Eq. (5). The notation $C(P)_{\text{stop}}$ indicates that the reference energy was gated on the stop detector. A timing asymmetry is observed, as indicated by the prompt centroids C_p obtained using the prompt ^{60}Co source and equal Compton energy gates (solid line). The horizontal dashed line is observed for an ideal γ – γ fast timing setup (symmetric timing).

The error of the calibrated centroid curve obtained from the evaluation of the covariance (error) matrix is 4–10 ps for the range of $200 \text{ keV} < E_\gamma < 1500 \text{ keV}$. This accuracy is in agreement with the measured centroid uncertainties and is representative for the goodness of the fit.

The prompt curve shown in Fig. 5 was obtained using the Compton continuum of the prompt ^{60}Co γ –ray source. In analogy to the measured full energy centroid curve, the stop detector was gated at 344 keV and the $\approx 10 \text{ keV}$ wide Compton gates were varied on the start detector. Over the total dynamic range, the obtained Compton centroids were fitted using Eq. (5). For $E_\gamma > 344 \text{ keV}$, the behavior of the calibrated centroid curve follows that of the approximated prompt curve and the shift between them is in the range of 33–61 ps. This is in good agreement with the known lifetime of 46.7(2.5) ps [12] of the 344 keV state when adopting a systematic error of 20 ps. However, in some regions non-monotonic timing behavior of the Compton events is observed. Especially for $E_\gamma < 344 \text{ keV}$, the shift between the centroid curve and the Compton events increases rapidly

with decreasing energy. Similar effects were observed in the timing analysis of the stop detector. It was already observed that a shift of the prompt spectra due to the full energy peaks in relation to those due to Compton events is obtained [2]. It is the effect of a contribution of a multiple Compton interaction in creation of full energy events that introduces a delay of a light pulse in relation to that due to the single Compton scattering [2]. This artificial delay is related to the time-of-flight of the scattered γ –rays which corresponds to 33 ps per cm and thus becomes important for large crystals like in our case.

Based on the fact that only full energy events reproduce the true prompt curve, the full energy centroids shown in Fig. 5 were corrected for the known lifetime of the 2_1^+ state in ^{152}Gd to calibrate the 344 keV gated prompt curve of the start detector. As presented in Fig. 6, an analogous centroid shift analysis was performed on the stop detector, where the reference 344 keV decay transition was gated on the start detector. The two

calibrated 344 keV gated prompt curves cross each other at nearly 344 keV which corresponds to the true PRF centroid of the setup for the combination 344–344 keV. This very good result indicates that the calibration function describes the two branch timing characteristics of our setup very well. However, the timing of the two branches is not symmetric, as can be seen in Fig. 6. This timing asymmetry results in an energy dependent prompt centroid for $\Delta E_\gamma = 0$ (equal energy gates), as illustrated by the data points obtained using the prompt ^{60}Co source and fitted with a straight line (solid line in Fig. 6).

To determine the PRF centroid for an energy combination of interest, more PRF information is needed. Using other reference energy gates, of course the resulting prompt curves differ from those presented in Fig. 6. This and the timing asymmetry of real fast timing setups makes the determination of the PRF centroid of interest complex. The proposed mirror symmetric centroid difference method, an extension of the centroid shift method, combines the two branch timing characteristics of a γ – γ fast timing setup and simplifies substantially the often difficult measurement of the prompt curve.

4. The mirror symmetric centroid difference (MSCD) method

In the previous section it was shown that in application of the γ – γ timing technique, the lifetime of a nuclear excited state can be measured either with the start branch or the stop branch detector. The problem of calibrating the prompt curve still remains, as the timing characteristics of the two branches differ in a real setup. Therefore, the prompt curve has to be calibrated for each branch. The timing asymmetry in the branch timing characteristics is canceled when defining a new physical quantity, the centroid difference

$$\Delta C = C(D)_{\text{stop}} - C(D)_{\text{start}}$$

for a specific γ –ray cascade in reference to Eq. (4) ($\tau = C(P) - C(D)$ when the decay transition is gated on the start). The obtained energy dependent prompt response difference,

$$\text{PRD} = C(P)_{\text{stop}} - C(P)_{\text{start}}$$

describes the combined γ – γ timing characteristics of the setup independent of the single branch timing characteristics.

We assume for simplification an ideal γ – γ fast timing setup, which means that both timing branches produce identical timing signals for identical energies, as presented in Fig. 7. In this example, we consider a decay transition with energy of 800 keV that is used as the walk free reference energy gate of the system. No background or feeding are contributing to the time distributions. Referring to Fig. 5, the centroid curve $C(D)_{\text{stop}}$ is shifted by $+\tau$ from the corresponding prompt curve $C(P)_{\text{stop}}$, as the decay transition, in that case used as the reference timing signal, is gated on the stop. If the decay transition is gated on the start detector, the corresponding centroid curve $C(D)_{\text{start}}$ is shifted by $-\tau$ from the prompt curve, as in this case the start detector is affected by the lifetime.

As can be seen in Fig. 7, one has to distinguish between $\Delta E_\gamma > 0$ and $\Delta E_\gamma < 0$, where ΔE_γ is the difference of the feeding and decaying γ –ray energies:

$$\Delta E_\gamma = E_{\text{feeder}} - E_{\text{decay}} \quad (6)$$

According to Eq. (4), the value of the centroid difference for both cases is given by

$$|\Delta C_{\text{decay}}| = \begin{cases} \text{PRD} + 2\tau : \Delta E_\gamma > 0 \\ \text{PRD} - 2\tau : \Delta E_\gamma < 0 \end{cases} \quad (7)$$

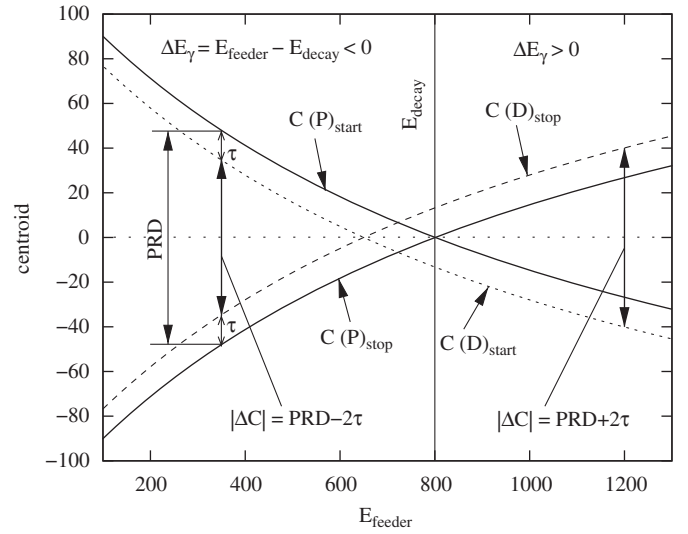


Fig. 7. The 800 keV gated prompt curves $C(P)$ of the two branches of an ideal fast timing setup with symmetric timing characteristics. The dashed curves are the centroid curves related to a lifetime τ obtained if only the decay transition is used as the reference energy gate (walk free timing signal of the system). Note that the relation for the centroid difference ΔC of the two delayed centroid curves depends on whether the feeding energy is larger or smaller than the decay energy.

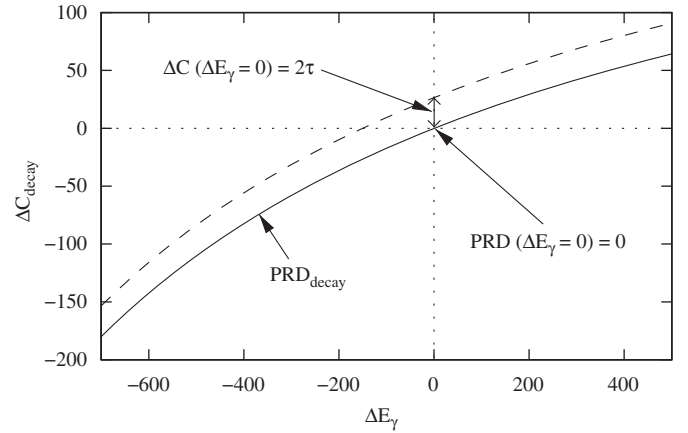


Fig. 8. The $(\Delta C, \Delta E_\gamma)$ –diagram: The energy dependent PRD describing the PRD curve (solid curve) of a γ – γ fast timing setup is obtained for a decay transition that is used as the reference energy gate of the setup. The combined centroid difference curve related to a lifetime τ (the dashed curve) is shifted from the PRD curve by $+2\tau$. The PRD curve crosses the zero point and therefore, the centroid difference at $\Delta E_\gamma = 0$ corresponds to 2τ .

while the centroid difference is defined as

$$\Delta C(\Delta E_\gamma)_{\text{decay}} = C(D)_{\text{stop}} - C(D)_{\text{start}} \quad (8)$$

The subscript “decay” indicates that the reference timing signal of the setup is provided by a decay transition, which in the case of “ $C(D)_{\text{stop}}$ ” is gated on the stop. Fig. 8 shows the linearly combined centroid difference curve obtained using Eq. (8) and plotted against the energy difference as defined in Eq. (6). Using Eq. (4), it follows:

$$\begin{aligned} \Delta C(\Delta E_\gamma)_{\text{decay}} &= C_P(\Delta E_\gamma)_{\text{stop}} + \tau - (C_P(\Delta E_\gamma)_{\text{start}} - \tau) \\ &= \text{PRD}(\Delta E_\gamma)_{\text{decay}} + 2\tau. \end{aligned} \quad (9)$$

In analogy to the standard centroid shift method, the linearly combined centroid difference curve (Eq. (9)) is shifted by $+2\tau$ from the corresponding PRD curve as illustrated in Fig. 8. The $(\Delta C, \Delta E_\gamma)$ –diagram is particularly useful because of the zero point

crossing of the PRD curve, that makes the direct determination of lifetimes possible, if the centroid difference at $\Delta E_\gamma = 0$ can be interpolated.

Now, we consider a feeding transition that is used as reference energy gate, i.e. the reference timing signal of the setup. Considering Fig. 7, the energy axis represents the decay energy. For the case of $E_{\text{feeder}} = 800 \text{ keV}$, the identical prompt curve $C(P)_{\text{stop}}$ is then obtained by gating the reference feeding transition on the stop detector. But, the resulting centroid curve $C(D)_{\text{stop}}$ is then shifted towards shorter times, because now the decay transition with its lifetime information is gated on the start detector. To account for this decay-feeder inversion which is equivalent to the start-stop inversion described by Eq. (7), we define the centroid difference for a reference feeding transition as

$$\begin{aligned} \Delta C(\Delta E_\gamma)_{\text{feeder}} &= C(D)_{\text{start}} - C(D)_{\text{stop}} \\ &= C_P(\Delta E_\gamma)_{\text{start}} + \tau - (C_P(\Delta E_\gamma)_{\text{stop}} - \tau) \\ &= \text{PRD}(\Delta E_\gamma)_{\text{feeder}} + 2\tau. \end{aligned} \quad (10)$$

Using Eqs. (6) and (8)–(10), the experimentally obtained centroid differences are well defined in the $(\Delta C, \Delta E_\gamma)$ -diagram. If we consider a cascade of two subsequent γ -rays with different γ -ray energies ($E_{\text{decay}} \neq E_{\text{feeder}}$) and the energy combination $\Delta E_{\text{casc.}} = E_{\text{feeder}} - E_{\text{decay}}$ as defined in Eq. (6), then Eqs. (9) and (10) are equivalent to

$$\Delta C(\Delta E_\gamma)_{\text{decay}} = \Delta C(\Delta E_\gamma)_{\text{feeder}} \quad (11)$$

$$\text{PRD}(\Delta E_\gamma)_{\text{decay}} = \text{PRD}(\Delta E_\gamma)_{\text{feeder}} \quad (12)$$

and accordingly

$$\text{PRD} = 0 \quad \text{and} \quad \Delta C = 2\tau \quad \text{for} \quad \Delta E_\gamma = 0. \quad (13)$$

Fig. 9 shows the (800 keV gated) $\text{PRD}_{\text{decay}}$ curve, as presented in Fig. 8, and the $\text{PRD}_{\text{feeder}}$ curve obtained when the reference energy gate corresponds to the feeding transition (Eq. (10)) of the investigated cascade, in this example with $E_{\text{feeder}} = 1190 \text{ keV}$. Note that the $\text{PRD}_{\text{feeder}}$ curve is convex, while the $\text{PRD}_{\text{decay}}$ curve is concave. As illustrated in Fig. 9, the relations of Eqs. (11)–(13) denote that for the specific energy combination $\Delta E_{\text{casc.}}$, the centroid difference (PRD) is independent of whether the reference energy gate corresponds to the energy of the feeding or the decaying transition. This is independent of the energy combination and thus the measurement of centroid differences cancels the timing asymmetry of the two timing branches in a real γ - γ fast timing setup.

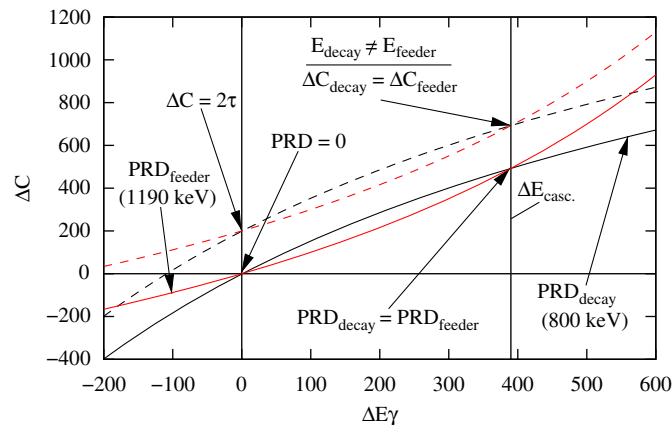


Fig. 9. The two centroid difference curves and corresponding PRD curves are obtained when the reference energy gate corresponds to the decay transition (800 keV) of a γ -ray cascade (e.g. $\text{PRD}_{\text{decay}}$), or to the feeding transition (Eq. (10)), respectively. Corresponding to the energy combination, the two curves cross each other at $\Delta E_{\text{casc.}} = E_{\text{feeder}} - E_{\text{decay}}$ and accordingly at $\Delta E_\gamma = 0$ (Eq. (13)).

The use of the MSCD method provides the following very advantageous features:

1. The zero point in the $(\Delta C, \Delta E_\gamma)$ -diagram can be used as a prompt calibration point, because Eq. (13) is independent of energy and timing characteristics of the two branches.
2. The time shift due to electronic drifts cancels, because this shift is independent of energy and therefore affects both time distributions in the same way.
3. Due to Eqs. (11) and (12), a centroid difference ΔC can be used twice, dependent on whether the feeding or the decaying transition is considered. This is very useful for the calibration of a PRD curve of interest.
4. Corollary, the total error for the calibration of the PRD curve is reduced.
5. Due to Eq. (13), one can determine picosecond lifetimes even without calibrating the PRD curve, if the combined timing characteristics is known. If enough data points for a reference feeding or decaying transition are available and one of these is near to the zero point, e.g. for $|\Delta E_\gamma| < 100 \text{ keV}$, the data points then can be fitted and the value of the centroid difference curve at $\Delta E_\gamma = 0$ is equal to 2τ .

In the majority of cases, the calibration of the PRD for an energy combination of interest is needed. Considering a specific reference energy gate which corresponds to the energy of a feeding transition ($\text{ref.} = E_{\text{feeder}} \Leftrightarrow \Delta E_\gamma = \text{ref.} - E_\gamma$), the PRD can be written as

$$\begin{aligned} \text{PRD}(-\Delta E_\gamma)_{\text{ref.} = E_{\text{feeder}}} &= C_P(E_\gamma - \text{ref.})_{\text{start}} - C_P(E_\gamma - \text{ref.})_{\text{stop}} \\ &= -(C_P(E_\gamma - \text{ref.})_{\text{stop}} - C_P(E_\gamma - \text{ref.})_{\text{start}}). \end{aligned} \quad (14)$$

For a decay transition that is used as reference signal, Eq. (6) is equivalent to $\Delta E_\gamma = E_\gamma - \text{ref.}$ and thus Eq. (14) is equivalent to

$$\text{PRD}(\Delta E_\gamma)_{\text{ref.} = E_{\text{decay}}} = -\text{PRD}(-\Delta E_\gamma)_{\text{ref.} = E_{\text{feeder}}} \quad (15)$$

$$\Delta C(\Delta E_\gamma)_{\text{ref.} = E_{\text{decay}}} = -\Delta C(-\Delta E_\gamma)_{\text{ref.} = E_{\text{feeder}}}. \quad (16)$$

These mirror symmetric relations imply that for a specific reference energy, the value of the centroid difference (PRD) is independent of whether this energy corresponds to the energy of the feeder or the decay. Thus, for a specific reference energy, Eq. (15) can be used to transform the PRD curve obtained for the reference energy as the decay energy into the PRD curve corresponding to the reference feeder of same energy.

5. Application of the MSCD method

The disadvantage of asymmetric timing in real γ - γ fast timing setups is compensated when determining the combined γ - γ timing characteristics for a combination of two detectors. Due to feeder-decay inversion, the PRD in the $(\Delta C, \Delta E_\gamma)$ -diagram is mirror symmetric which makes the calibration of the PRD for any energy combination possible. In particular cases, the mirror symmetric representation of centroid differences allows for direct lifetime determination. For both purposes, the PRD curve of the setup has to be determined.

5.1. The direct picosecond lifetime determination

Referring to the prompt curve calibration described in Section 3, we again consider the first 2^+ state in ^{152}Gd . The 344 keV decay transition is used as the reference signal to measure the centroid difference curve of the setup. As illustrated in Fig. 10, the centroid (time) difference of the two centroids obtained for a specific

γ -ray cascade by gating the detectors in the two possible ways is measured. This is made for every combination of the 344 keV decay transition with a coincident feeding transition. In our case, the 344 keV transition is used as the reference decay transition and according to Eqs. (6) and (8), the resulting centroid differences are plotted in the $(\Delta C, \Delta E_\gamma)$ -diagram, as presented in Fig. 11. If an intermediate state was involved in the measurement, the obtained centroid difference is corrected by twice the lifetime of the intermediate state.

Assuming Eq. (5) to describe the two branch timing characteristics of our setup, the linearly combined timing characteristics should follow the same E_γ or ΔE_γ dependency, as the decay energy $E_{\text{decay}} = 344$ keV is kept constant. Hence, the centroid differences shown in Fig. 11 and connected by the dashed curve are fitted with

$$\Delta C = \frac{a}{\Delta E_\gamma + b} + c. \quad (17)$$

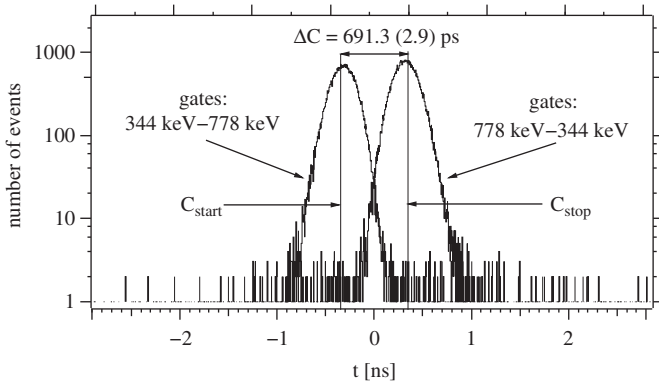


Fig. 10. Time spectra of the 778→344 keV cascade obtained by gating the detectors in both ways. The centroid obtained by gating the decay transition on the start branch is indicated with C_{start} . The statistical error for the centroid difference ΔC is calculated as $d(\Delta C) = \sqrt{(dC_{\text{start}})^2 + (dC_{\text{stop}})^2}$ with dC according to Eq. (3).

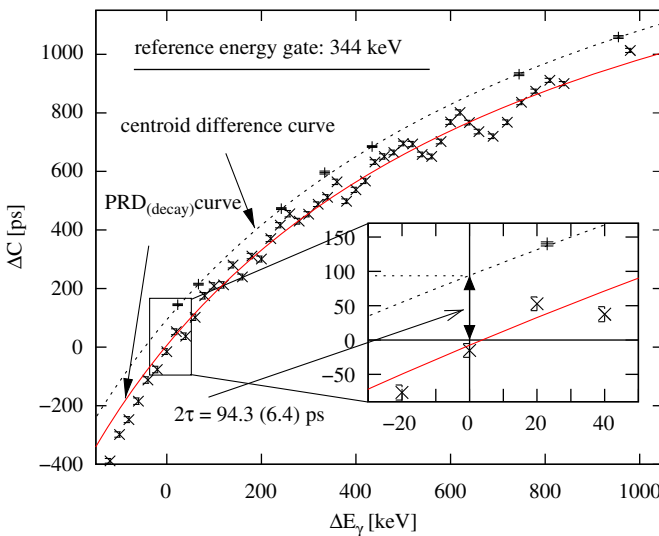


Fig. 11. The $(\Delta C, \Delta E_\gamma)$ -diagram: The dashed curve was obtained by a fit of the 344 keV gated centroid differences ΔC as a function of the energy difference (Eq. (17)). Also shown are the 344 keV gated centroid differences obtained using the Compton continuum of the prompt ^{60}Co source. Inset: The value of the centroid difference curve at $\Delta E_\gamma = 0$ corresponds to twice the lifetime of the 2_1^+ state in ^{152}Gd .

The fit parameters obtained are

$$a = -(2239 \pm 175) \times 10^3 \text{ keV ps} \quad (7.8\%)$$

$$b = (1091 \pm 54) \text{ keV} \quad (5.0\%)$$

$$c = (2056 \pm 62) \text{ ps} \quad (3.0\%).$$

As expected, the calibration function (Eq. (17)) fits every data point, but now within the statistical errors $d(\Delta C)$ of only 3–10 ps. Moreover, the interpolation of the centroid difference at $\Delta E_\gamma = 0$ gives a value of $2\tau = 94.3(6.4)$ ps which is in excellent agreement with the known lifetime of 46.7(2.5) ps [12].

For comparison, also the 344 keV gated centroid differences of Compton events from the prompt ^{60}Co source are shown in Fig. 11. The fit of the Compton centroid differences (the solid curve) with Eq. (17) represents the approximated 344 keV gated PRD curve, that crosses the zero point within < 6 ps. The fit was performed for $\Delta E_\gamma > 0$ and the resulting PRD curve is nearly parallel to the calibrated centroid difference curve. However, due to non-monotonic behavior of the Compton data points, the error of the PRD curve obtained from the covariance matrix is 20–40 ps for $200 \text{ keV} < E_\gamma < 1500 \text{ keV}$ compared with only 6–12 ps for the 344 keV gated full energy centroid difference curve.

5.2. The PRD calibration procedure

The best procedure to measure the PRD curve is to use full energy events. Therefore, the full energy centroid differences presented in Fig. 11 were corrected by twice the known lifetime of the 344 keV state in ^{152}Gd to obtain the 344 keV gated PRD curve. But we need more PRD information to calibrate the PRD for an energy combination of interest. Fortunately, beside ^{152}Gd , the standard ^{152}Eu source also produces ^{152}Sm after electron capture decay. As can be seen from the decay scheme in Fig. 12, four transitions are in coincidence with the 244 and the 444 keV transitions which therefore can be used as reference energy gates to obtain more PRD informations for the same experimental situation. MSCD analyzes were performed on the 244 and the

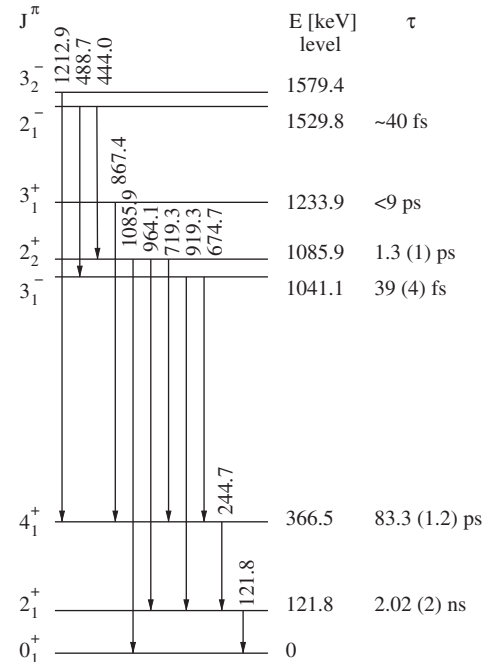


Fig. 12. Partial level scheme of ^{152}Sm obtained after electron capture decay of ^{152}Eu . J^π , E_{level} , E_γ and τ from Ref. [12].

444 keV transitions in ^{152}Sm , whereby the centroid differences of coincident transitions were corrected for corresponding known lifetimes.

As presented in Fig. 13 (see also Fig. 12), the 444 keV transition is used as the reference feeding transition and thus the corresponding PRDs are plotted in the $(\Delta C, \Delta E_\gamma)$ -diagram according to Eqs. (6) and (10). Accordingly (Eq. (12)), the measured PRD for the combination 444–244 keV at $\Delta E_\gamma = 200$ keV is used for fitting both the 244 and the 444 keV gated PRD curves. To investigate the quality of the fits, a data point is added at the zero point. Within < 7 ps, the calibrated PRD curves cross the zero point. Independent of the reference energy gate, the calibration function describes the combined timing characteristics of our setup remarkably well. Obviously, the best fit is obtained for the 344 keV gated PRD curve (the solid curve).

In Fig. 14, the PRDs for the combinations 244–344 and 444–344 keV interpolated from the 344 keV gated PRD_{decay} curve are compared with those interpolated from the other two

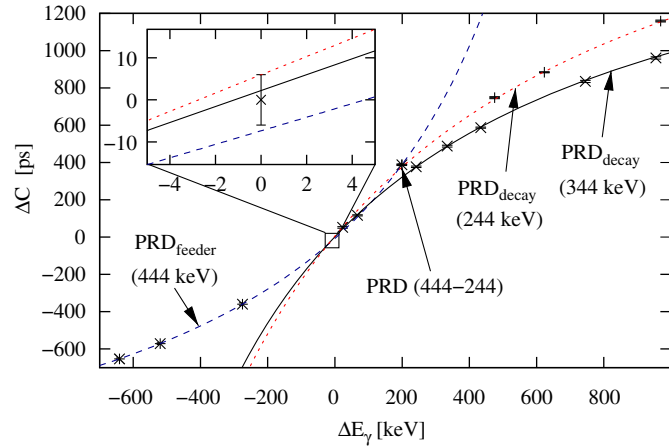


Fig. 13. PRD curves for different reference energy gates obtained by a fit of the corresponding PRDs (data points) using Eq. (17). For comparison, a data point with average error of 6 ps is added at the zero point (PRD = 0 for $\Delta E_\gamma = 0$).

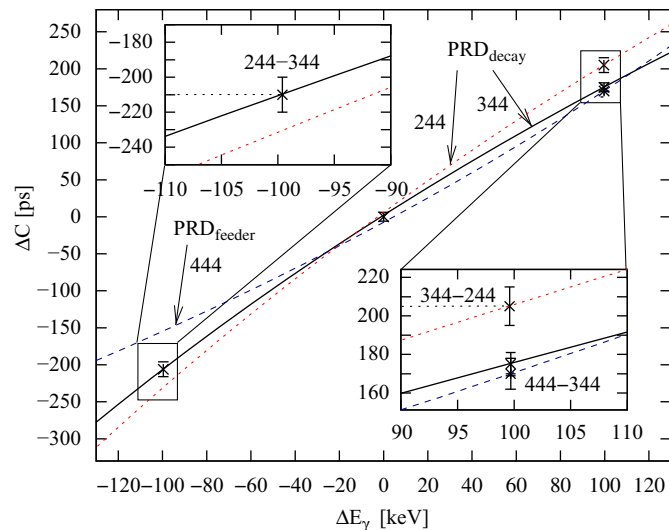


Fig. 14. Zoomed portions of the $(\Delta C, \Delta E_\gamma)$ -diagram presented in Fig. 13. According to Eq. (12), the 444 keV gated PRD_{feeder} curve should cross the 344 keV gated PRD_{decay} curve at $\Delta E_\gamma = +100$ keV. The values of the PRDs obtained for same energy combinations but interpolated from different PRD curves are in agreement within the statistical errors. The mirror symmetry of PRDs (Eq. (15)) is a result of feeder-decay inversion.

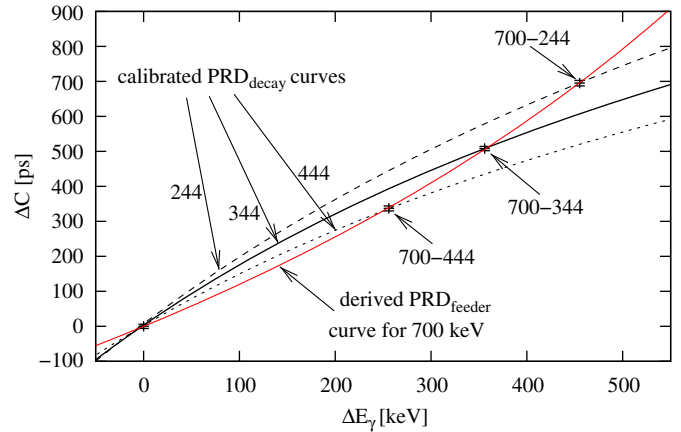


Fig. 15. Illustration of the PRD calibration procedure: The three PRD curves for referring decay energies were calibrated using background corrected full energy centroid differences. The PRDs for the energy of interest (700 keV) are interpolated from these three curves. The obtained PRDs including the zero point are used to calibrate the PRD curve of interest, in this case for the reference feeding energy of 700 keV.

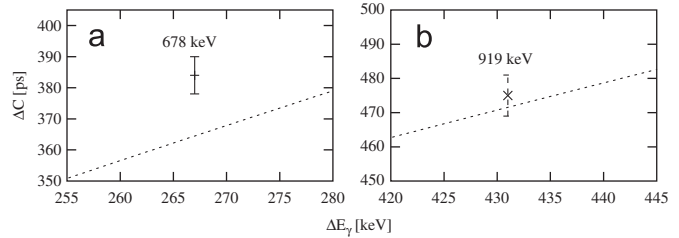


Fig. 16. (a) Background corrected centroid difference of the sequence 678→411 keV. The dashed line shows the calibrated 411 keV PRD_{decay} curve. The shift between the data point and the PRD curve is twice the lifetime of the 755 keV state in ^{152}Gd . (b) Background corrected centroid difference of the sequence 488→919 keV and the calibrated 488 keV PRD_{decay} curve.

Table 1

Lifetime results obtained from the MSCD method using background corrected centroid differences.

Nucleus	State J^π	E_{level} (keV)	E_γ (keV)	τ_{MSCD} (ps)	$\tau_{\text{Lit.}}$ (ps)
^{152}Sm	4_1^+	366.5	244.7	84.5(6.6)	83.3(1.2)
	2_2^+	1085.9	444.0 ^a	2.5(3.9)	1.3(0.1)
	3_1^-	1041.1	919.3	$< 4^b$	0.039(6)
^{152}Gd	2_1^+	344.3	344.3	47.1(3.2)	46.7(2.5)
	4_1^+	755.4	678.6	11.2(3.8) ^c	10.5(0.6)

The lifetimes were deduced from the value of the calibrated centroid difference curve at $\Delta E_\gamma = 0$, except cases b and c as noticed below.

^a Used as reference feeder with Eq. (10).

^b Result obtained from the shift to the 488.7 keV PRD curve (Fig. 16b).

^c Result obtained from the shift to the 411.1 keV PRD curve (Fig. 16a).

PRD curves. Within < 6 ps, the results are in agreement, which is another strong indication that the calibration function defines the combined timing characteristics of our setup. Small deviations can be explained by the low number of PRDs used to calibrate the 244 and the 444 keV gated PRD curves, but also by background contributions which might shift the true PRD.

A MSCD analysis to correct the PRDs for background contributions was performed on all transitions involved in this work, as described in Section 5.3. Fig. 15 shows the final PRD curves after corrections for background and including the zero point and other

PRDs obtained from the best fitted 344 keV PRD curve. For a simplified illustration of the PRD calibration procedure, the 444 keV PRD curve as presented in Fig. 13 is mirrored with respect to the origin (Eq. (15)). From these three PRD_{decay} curves for corresponding reference decay energies, one interpolates the PRD for the energy of interest, which in this example corresponds to a feeder of 700 keV. Including the zero point, the obtained PRDs are then fitted using Eq. (17) to calibrate the 700 keV gated PRD_{feeder} curve, of which one can interpolate the PRD for the decay energy of interest. In total, after corrections for background and including additional calibration points, the resulting error of the PRD determination for any energy combination in the range of 200 keV < E_γ < 1500 keV is only 4–8 ps (∝ 2Δτ).

For lifetime determination of the 755 keV state in ¹⁵²Gd, the PRD curve was calibrated for the 411 keV decay transition, as explained before. Fig. 16a shows the 411 keV PRD curve and the background corrected data point of the direct feeder with 678 keV. Analogous, the MSCD result of the lifetime determination of the 1041.1 keV state in ¹⁵²Sm is presented graphically in Fig. 16b. The final lifetime results obtained using the MSCD method after corrections for background are presented in Table 1.

5.3. The background correction procedure

In γ-ray spectroscopy the full energy peaks of interest are sitting on the Compton distributions which are caused by γ-rays of higher energies. Using a compact detector array, also cross-talk events and scattered γ-rays from the surrounding can play a role. Using active Compton shielding, the background is remarkably reduced, but still some amount of background is obtained, as part of this background is generated from coincident γ-rays. The obtained time distribution is a superposition of the time spectra due to full energy events and due to Compton events of same energy, i.e. the background underneath the full energy peak. The Compton time distribution of interest can be interpolated by the measurements of Compton time spectra at different energies in the region around the transition of interest [1,2]. For the MSCD method, the procedure is analogous, but the centroid difference of the two Compton time distributions obtained from each branch for a certain energy combination is measured instead. Such an analysis is presented in Fig. 17, where the 244 keV full energy

peak was used as the reference energy gate and the Compton gates were varied in the range of 270–820 keV.

Except for a few points, the overall behavior the Compton centroid differences is smooth. However, for ΔE_γ < 130 keV, a large change of the shift between the Compton events and the full energy centroid difference curve is observed. Therefore, the Compton data points were fitted for ΔE_γ > 130 keV, as shown in the inset of Fig. 17. The interpolated shift t_s = ΔC_T – ΔC_C between the (total) full energy centroid difference at ΔE_γ = 200 keV and the Compton centroid difference curve is t_s = 12(6) ps. As a linear combination of centroids, the total centroid difference can be written as the sum of the true delayed (or prompt) centroid difference ΔC_D and the Compton centroid difference ΔC_C

$$\Delta C_T = \frac{\Delta C_D + \alpha \Delta C_C}{1 + \alpha} = \Delta C_D + t_c \quad (18)$$

where α is the relative background intensity or the background to full energy ratio, respectively. Eq. (18) is only valid, if the two branches have the same peak to background ratio, which was approximately the case in our experiment. We used the mean value obtained from the two branches and adopted a systematic error of 10% which is overestimated. To obtain the correction term t_c, Eq. (18) is equivalent to

$$t_c = \Delta C_T - \Delta C_D = -\alpha(\Delta C_T - \Delta C_C) = -\alpha t_s \Leftrightarrow \Delta C_D = \Delta C_T + \alpha t_s. \quad (19)$$

Due to bad peak to background ratio of 1.25 for the 444 keV transition obtained from the 244 keV gated coincidence spectrum, the total centroid difference ΔC_T of the 444–244 keV combination has to be corrected by +9.6(4.0) ps. This result can be verified by a MSCD analysis of the other full energy peak of the investigated 444–244 keV centroid difference, the feeding 444 keV transition, as shown in Fig. 18. In this case, the fit of the Compton centroid differences was performed for ΔE_γ < 40 keV and the centroid difference for the combination 244–444 keV is shifted by +71(7) ps from the Compton centroid difference curve. According to the peak to background ratio of 6.5 for the 244 keV transition, the Compton shift at ΔE_γ = –200 keV results in a correction of +11(1) ps which is in very good agreement with the previously determined correction. Analogous studies were made for all γ-rays involved in lifetime determination for this work. Due to very good peak to background ratios, the corrections for background are in the range of only 0–6 ps and the resulting additional error is smaller than 1 ps, thus negligibly small.

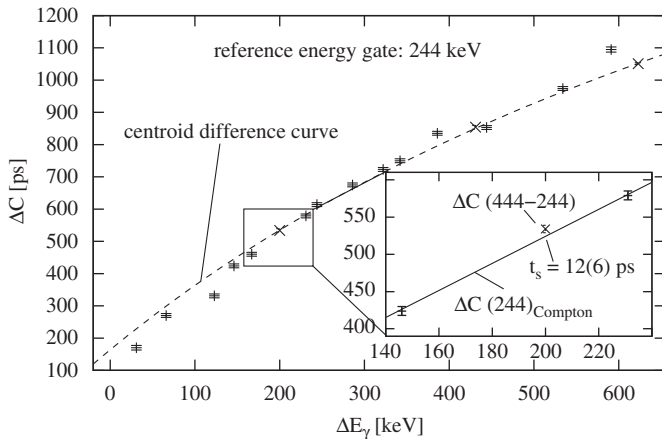


Fig. 17. 244 keV gated Compton centroid differences (ΔC(244)_{Compton}) compared with the full energy 244 keV gated centroid difference curve of the 4⁺ state in ¹⁵²Sm. Inset: For ΔE_γ > 130 keV, the Compton data points (boxes) were fitted using Eq. (17) (the solid curve). A significant shift t_s between the Compton centroid difference curve and the full energy centroid difference at ΔE_γ = 200 keV is observed.

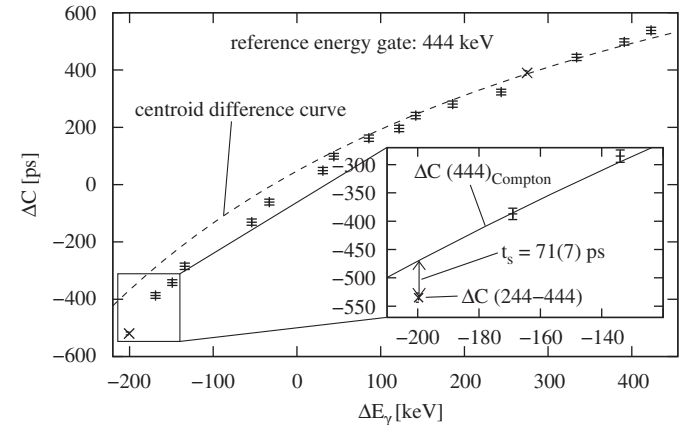


Fig. 18. MSCD analysis of Compton centroid differences using the 444 keV transition as the reference energy gate of the setup. Inset: the Compton centroid difference curve was obtained by a fit of the Compton data points with ΔE_γ < 40 keV.

6. Conclusion

In the case of full energy events, an E_γ dependency of the fast timing signal has been established, measured and used to correct the experimental data. This dependency will be verified by systematic prompt curve and PRD curve measurements using different timing adjustments and also different scintillators and photomultipliers.

The powerful mirror symmetric centroid difference method makes the determination of picosecond lifetimes of nuclear excited states easier and more precise. Using this new method picosecond lifetimes are determined directly in cases where the nuclear excited state is fed or decays by several γ -rays. The value of the centroid difference curve $\Delta C(\Delta E_\gamma)$ at $\Delta E_\gamma = 0$ is then twice the lifetime of the considered nuclear excited state.

The identification of the timing characteristics of our experimental setup has brought forth a high precision γ - γ timing calibration procedure. Due to mirror symmetry of centroid differences (PRDs) and the universal prompt calibration point at the zero point, additional data points are obtained for a more precise PRD curve calibration. The PRD curve is calibrated as a function of energy for any energy combination in the range of 200–1500 keV with an accuracy of 4–8 ps resulting in a lifetime determination limit of 2–4 ps. This limit is a little increased by statistical uncertainties of the centroid determinations. For good peak to background ratios of more than 5, the additional error

induced by the described background correction procedure is smaller than 1 ps, thus often negligible.

Acknowledgements

The author would like to thank Dr. H. Mach, Dr. G. Simpson and especially Dr. P. Petkov for valuable discussions. The LaBr₃(Ce) scintillator detectors were financed by the BMBF under Contract 06KY2051. Part of this work was financially supported by the F&E of the GSI under Contract KJOLIE and by the BMBF under Contract 06KY9136I.

References

- [1] H. Mach, et al., Nucl. Instr. and Meth. A 280 (1989) 49.
- [2] H. Mach, et al., Nucl. Phys. A 523 (1991) 197.
- [3] M. Moszyński, et al., Nucl. Instr. and Meth. A 277 (1989) 407.
- [4] M. Moszyński, et al., Nucl. Instr. and Meth. A 567 (2007) 31.
- [5] W. Andrejtscheff, et al., Nucl. Instr. and Meth. A 204 (1982) 123.
- [6] P. Petkov, et al., Nucl. Instr. and Meth. A 321 (1992) 259.
- [7] A. Iltis, et al., Nucl. Instr. and Meth. A 563 (2006) 359.
- [8] B. Bengston, M. Moszyński, Nucl. Instr. and Meth. A 204 (1982) 129.
- [9] E.R. White, et al., Phys. Rev. C 76 (2007) 057303.
- [10] J.-M. Régis, et al., Nucl. Instr. and Meth. A 606 (2009) 466.
- [11] T.J. Paulus, IEEE Trans. Nucl. Sci. NS-32/3 (1985) 1242.
- [12] National Nuclear Data Center, <www.nndc.bnl.gov>.